Isothermal Titration Calorimetry Studies of the Binding of a Rationally Designed Analogue of the Antimicrobial Peptide Gramicidin S to Phospholipid Bilayer Membranes†

Thomas Abraham,‡ Ruthven N. A. H. Lewis,‡ Robert S. Hodges,# and Ronald N. McElhaney*,‡

Department of Biochemistry, University of Alberta, Edmonton, Alberta, Canada T6G 2H7, and Department of Biochemistry and Molecular Genetics, University of Colorado Health Sciences Center at Fitzsimons, Aurora, Colorado 80045

Received September 7, 2004; Revised Manuscript Received November 23, 2004

ABSTRACT: The binding of the positively charged antimicrobial peptide cyclo[VKL*d*KV*d*YPLKVKL*d*YP] (GS14*d*K4) to various lipid bilayer model membranes was investigated using isothermal titration calorimetry. GS14*d*K4 is a diastereomeric lysine ring-size analogue of the naturally occurring antimicrobial peptide gramicidin S which exhibits enhanced antimicrobial and markedly reduced hemolytic activities compared with GS itself. Large unilamellar vesicles composed of various zwitterionic (1-palmitoyl-2-oleoyl-*sn*-glycero-3-phosphorylcholine [POPC]) and anionic phospholipids {1-palmitoyl-2-oleoyl-*sn*-glycero-3-[phospho-*rac*-(glycerol)] [POPG] and 1-palmitoyl-2-oleoyl-*sn*-glycero-3-[phosphoserine] [POPS]}, with or without cholesterol, were used as model membrane systems. Dynamic light scattering results indicate the absence of any peptide-induced major alteration in vesicle size or vesicle fusion under our experimental conditions. The binding of GS14*d*K4 is significantly influenced by the surface charge density of the phospholipid bilayer and by the presence of cholesterol. Specifically, a significant reduction in the degree of binding occurs when three-fourths of the anionic lipid molecules are replaced with zwitterionic POPC molecules. No measurable binding occurs to cholesterol-containing zwitterionic vesicles, and a dramatic drop in binding is observed in the cholesterol-containing anionic POPG and POPS membranes, indicating that the presence of cholesterol markedly reduces the affinity of this peptide for phospholipid bilayers. The binding isotherms can be described quantitatively by a one-site binding model. The measured endothermic binding enthalpy (ΔH) varies dramatically (+6.3 to +26.5 kcal/mol) and appears to be inversely related to the order of the phospholipid bilayer system. However, the negative free energy (ΔG) of binding remains relatively constant (−8.5 to −11.5 kcal/mol) for all lipid membranes examined. The relatively small variation of negative free energy of peptide binding together with a pronounced variation of positive enthalpy produces an equally strong variation of $T\Delta S$ (+16.2 to +35.0 kcal/mol), indicating that GS14*d*K4 binding to phospholipids bilayers is primarily entropy driven.

The binding of water-soluble peptides or proteins to lipid membranes is an important issue in many biological processes. There are, for instance, several types of amphipathic peptides, including gramicidin S (GS),[1] that bind to the bacterial membrane and act as antibiotics (*1*, *2*). These antimicrobial peptides are widely distributed in animals and plants where they act as host defense peptides. Most of these antimicrobial peptides are cationic, thus permitting electrostatic interactions with the bacterial cytoplasmic membrane, which usually contains substantial amounts of negatively charged phospholipids in the outer leaflet of the lipid bilayer, the major target of many of these peptides.

GS, a cyclic decameric cationic antimicrobial peptide first isolated from the Gram-positive bacteria *Bacillus brevis*, is one of a series of antimicrobial peptides produced by this particular organism (*3*). The GS molecule, of primary structure (cyclo[VOL*d*FPVOL*d*FP]), is composed of a double-stranded antiparallel β-sheet connected by a pair of II′ β-turns (*3*). GS is a powerful antibiotic against a broad range of Gram-negative and Gram-positive bacteria as well as several pathogenic fungi, but it is also highly hemolytic

† Supported by operating grants from the Canadian Institutes of Health Research (R.N.M.), major equipment grants from the Alberta Heritage Foundation for Medical Research (R.N.M.), Grants RO1 AI148714 and RO1 GM61855 from the National Institutes of Health (R.S.H.) and the John Stewart Chair in Peptide Chemistry (R.S.H.).

* Corresponding author: Telephone: (780) 492-2413. Fax: (780) 492-0095. E-mail: rmcelhan@ualberta.ca.

‡ University of Alberta.

University of Colorado Health Sciences Center at Fitzsimons.

[1] Abbreviations: GS, gramicidin S, cyclo[VOLdFPVOL*d*FP] (the amino acid immediately after *d* is the D-enantiomer); GS14, gramicidin analogue, cyclo[VKLKV*d*YPLKVKL*d*YP]; GS14*d*K4, gramicidin analogue, cyclo[VKL*d*KV*d*YPLKVKL*d*YP]; POPC, 1-palmitoyl-2-oleoyl-*sn*-glycero-3-phosphorylcholine; POPG, 1-palmitoyl-2-oleoyl-*sn*-glycero-3-[phospho-*rac*-(glycerol)] (sodium salt); POPS, 1-palmitoyl-2-oleoyl-*sn*-glycero-3-[phosphoserine] (sodium salt); FTIR, Fourier transform infrared spectroscopy; ITC, isothermal titration calorimetry; MLV, multilamellar vesicle; LUV, large unilamellar vesicle; ΔH, total binding enthalpy; ΔG, free energy of binding; ΔS, entropy of binding; h_i, heat of reaction per injection; $h_{d,i}$, heat of dilution; *d*, hydrodynamic diameter; X_b^i, degree of binding, fraction of bound peptide per mole of total lipid; c_f^i, concentration of the peptide remaining free in solution after *i* injection; K_c^i, concentration-dependent binding constant; K_d, equilibrium dissociation constant; *E*, internal energy; *A*, surface area; k^{-1}, Debye length; *S*, entropy; π, surface pressure; α, area expansivity at constant membrane tension; χ, isothermal area compressibility or lateral compressibility.

10.1021/bi048077d CCC: $30.25
Published on Web 01/19/2005

(*4*−*7*). As a result, the use of this antimicrobial peptide is restricted to topical applications. However, a dissociation of the antimicrobial and hemolytic activities of GS is possible by simultaneously varying both GS ring size and the enantiomeric configuration of certain amino acid residues (*5*, *6*). This opens the possibility of the use of structural analogues derived from GS as an injectable or oral antibiotics (*4*, *8*).

GS14*d*K4 is a GS analogue that has been identified as a promising candidate because of its comparable antimicrobial activity to that of GS and its substantially lower hemolytic activity, which is about 15−20-fold less than that of GS (*6*). This analogue consists of two antiparallel β-sheets with aligned sequences of alternating hydrophobic and cationic residues, Val-Lys-Leu-*d*Lys-Val and Val-Lys-Val-Lys-Leu, connected at each end of the ring by the dipeptide sequence *d*Tyr-Pro. Thus, as the structure indicates, it is a diastereomeric analogue of GS14 in which the L-lysine at position 4 is substituted by its diastereomer, D-lysine. In the parent compound GS14, all four lysine units project to the one hydrophilic face of the ring, while in GS14*d*K4, the Lys-4 projects partially to the hydrophobic face of the molecule (*8*). This makes GS14*d*K4 relatively more water soluble, less amphiphilic, and less susceptible to dimerization than GS14 itself (*8*).

The interaction between GS14*d*K4 and lipid bilayer model membranes has been studied using FTIR spectroscopy in an effort to understand the basis of its capacity to differentiate between bacterial and mammalian cell membranes (*9*). The FTIR data show that GS14*d*K4, like GS, interacts more strongly with anionic lipid bilayers than with zwitterionic, uncharged, or cationic lipid model membranes. The interaction of GS14*d*K4 with such model membranes is, however, generally weaker than with GS and depends more strongly on the charge of the bilayers. Moreover, GS14*d*K4, like GS, interacts more strongly with liquid crystalline lipid bilayers than with gel-state lipid bilayers. In addition, GS14*d*K4 is essentially completely excluded from cholesterol-containing zwitterionic lipid membranes, whereas cholesterol only attenuates the interactions of GS with such lipid bilayers (*10*). GS14*d*K4, despite its apparently weaker interactions with phospholipid membranes, is more effective in permeabilizing cholesterol-free lipid membranes than GS (*11*). These observations suggest that GS14*d*K4 retains the ability to disrupt bacterial membranes as effectively as GS because of its innately greater ability to disrupt lipid bilayers and its retained selectivity for binding to anionic lipids, but exhibits much weaker hemolytic activity because of its exclusion from cholesterol-containing zwitterionic lipid membranes.

Although these semiquantitative studies of the interaction between GS14*d*K4 and the various model lipid membranes were valuable, there is a clear need for a quantitative determination of the degree of binding of the GS14*d*K4 to various types of lipid bilayers and for a comprehensive thermodynamic description of the binding process. A quantitative determination of peptide binding to various types of lipid membranes is particularly important as it would allow us determine the amount of the peptide actually present in the membrane as opposed to the amount of added peptide in the aqueous solution. Similarly, a complete thermodynamic description of the binding process would provide key information on the energetics and mechanism of peptide binding to lipid bilayers. We have therefore utilized ITC, a highly sensitive tool for determining the binding of peptide to lipid membranes (*12*, *13*), to examine the binding of GS14*d*K4 to large unilamellar vesicles (LUVs) composed of various zwitterionic and anionic phospholipids, with or without cholesterol. The degree of binding and the thermodynamic parameters of binding obtained for these different lipid compositions were compared and analyzed to understand the nature of the interactions involved in the binding process.

MATERIALS AND METHODS

Materials. All phospholipids and cholesterol were obtained from Avanti Polar Lipids Inc. (Alabaster, AL) and used without further purification. The linear peptide sequence VKL*d*KV*d*YPLKVKL*d*YP, where *d* denotes a D-amino acid residue, was synthesized by solid-phase peptide synthesis using *tert*-butyloxycarbonyl chemistry. The linear peptide was then N- to C- (Pro at the C-terminus) terminally cyclized in solution to produce GS14*d*K4 (*4*−*6*). Both the linear and cyclic peptides were purified and analyzed by RP-HPLC, and their final purity was determined by mass spectrometry. The concentration of the pure peptides in aqueous stock solutions was determined by amino acid analysis with a range of error ± 5%. All experiments, unless otherwise stated, were conducted in a buffer solution containing 50 mM Tris, 150 mM NaCl, and 1 mM NaN_3, pH 7.4.

Preparation of LUVs. The single-component lipid vesicles were prepared as follows. In a typical experiment, defined amounts of lipid (∼120 mg) were first dried under reduced pressure (vacuum) overnight. The lipid was then hydrated with a definite amount of buffer (∼4 mL) and the dispersion thus formed was subjected to vortex mixing at temperatures well above the gel/liquid crystalline phase transition temperature of the phospholipids. The MLVs thus obtained were then freeze−thawed several times. The MLVs were then extruded through a small volume extrusion apparatus (Avestin Inc., Ottawa, Canada) equipped with a polycarbonate membrane filter (19 mm diameter, 200 nm pore diameter) about 25 times, to produce LUVs of vesicle size ∼200 nm. The vesicle size was later confirmed by dynamic light scattering measurements (see below for details). Lipid concentrations were determined by gas chromatography using an appropriate internal standard (± 5% error). The same procedure was followed for two-component vesicles, except that appropriate quantities of each component (lipid or cholesterol) were first co-dissolved in chloroform and thoroughly mixed prior to vesicle preparation.

High-Sensitivity Isothermal Titration Calorimetry. The heat flow resulting from the binding of the peptide to lipid vesicles was measured using a high-sensitivity VP-ITC instrument (Microcal LLC, Northampton, MA), with a reaction cell volume of 1.4448 mL. Prior to use, solutions were degassed under vacuum (140 mbar, 8 min) to eliminate air bubbles. The data were acquired by computer software developed by MicroCal LLC. Titration calorimetric experiments were used in two different modes (*12*). In the first mode, the peptide solution (25−50 μM) was placed in the calorimeter cell and the lipid vesicles (4−45 mM) were injected via the titration syringe in aliquots of 5−10 μL. Each injection produced a heat of reaction, h_i, which was

Table 1: Hydrodynamic Diameter of Pure and the Peptide-Bound LUVs

model membrane	hydrodynamic diameter (*d*), nm	
	in buffer	in GS14*d*k4 solution
POPC	166	168
POPG	178	199
POPS	176	178
POPC/POPG (3:1)	179	180
POPC/POPS (3:1)	180	183
POPG/cholesterol (6:4)	195	208
POPS/cholesterol (6:4)	179	188

determined by integration of the heat flow tracings. In the event of complete binding, this mode is capable of providing both the binding isotherm and the total binding enthalpy. In the case of an incomplete binding isotherm (e.g., POPC vs GS14*d*K4), the total binding enthalpy cannot be determined in the same manner. Therefore, the titration experiments were performed in the second mode, where the calorimeter cell was filled with lipid vesicles (~10 mM) and the peptide (100 μM) was injected into the calorimeter cell in aliquots of 10 μL. Under these conditions, the lipid is much in excess over the peptide during the whole titration experiment. Each injection should thus produce the same heat of reaction, h_i, from which the total binding enthalpy, ΔH, could be determined (*12*, *14*).

The heat of dilution, $h_{d,i}$, was determined in control experiments by injecting the corresponding vesicle dispersion (or peptide solution) into the buffer solution. The heats of dilution were subtracted from the heats determined in the corresponding peptide−lipid binding experiments. Thus, the quantitative evaluation of the experimental data was based on the relationship, $\Delta h_i = h_i - h_{d,i}$. The overall binding enthalpy and the binding isotherm were determined from these peptide−lipid binding experiments using standard procedures (*12*). In this study, since we do not have any direct experimental evidence to establish the transmembrane distribution of peptide molecules, we used the total lipid concentration in the estimation of the degree of binding and the determination of the thermodynamic binding parameters.

Dynamic Light Scattering. The average hydrodynamic diameter of pure and peptide-bound LUVs were measured by a Brookhaven BI-90 particle analyzer (Brookhaven Instruments, Holtsville, NY) using disposable square cells. The solutions were subjected to scattering by a monochromatic light (10 mW He−Ne laser, wavelength = 632.4 nm) and the scattered light intensity was measured at a scattering angle of 90°.

RESULTS

Size of Pure and Peptide-Bound LUVs. It has been reported previously that GS itself may cause phospholipid vesicle fusion and lysis and remove lipid from human erythrocyte membranes, at least at high concentrations of peptide (*1*). Thus, to check the integrity of the LUVs exposed to GS14*d*K4, the DLS measurements were performed on both control vesicles (LUVs titrated into buffer solution without peptide) and the sample vesicles (LUVs titrated into the peptide-containing buffer). The data are summarized in Table 1. Although the hydrodynamic diameters (*d*) of the peptide-bound lipid vesicles are marginally higher than those of pure lipid vesicles, these results indicate that the various lipid vesicles remain largely intact and do not undergo extensive fusion in the presence of the antimicrobial cyclic peptide GS14*d*K4 under the experimental conditions employed in our ITC measurements.

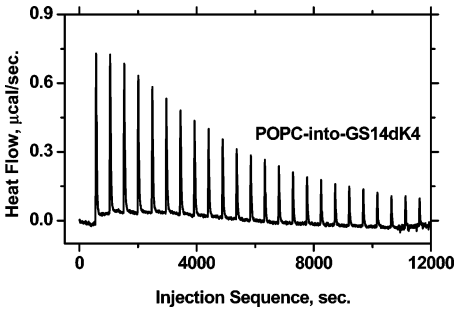

FIGURE 1: ITC experimental data at 25 °C. 10 μL aliquots of POPC LUVs (45 mM) were repeatedly injected into the reaction cell (1.4448 mL) containing GS14*d*K4 (50 μM). Each peak refers to the injection. Each injection produced an endothermic heat of reaction which decreased in magnitude with subsequent injections. The binding appears to be incomplete, even after 25 lipid injections of 10 μL aliquots of these POPC vesicles.

Binding of GS14dK4 to Zwitterionic POPC LUVs. Figure 1 illustrates an ITC experiment in which 10 μL aliquots of 1-palmitoyl-2-oleoyl-*sn*-glycero-3-phosphorylcholine (POPC) LUVs (45 mM) were repeatedly injected into the reaction cell containing GS14*d*K4 (50 μM). Each injection produced an endothermic heat of reaction which decreased in magnitude with subsequent injections. As the titration continues, the heat flow decreases. This is because after each addition of lipid, peptide is bound to the lipid vesicles and removed from bulk solution and hence less and less peptide is available for binding to the lipid vesicles subsequently injected. In the course of the titration, the free peptide concentration in the calorimeter cell decreases from 50 μM at the beginning of the titration to ~20 μM after 25 lipid injections. The binding appears to be very weak and incomplete even after 25 lipid injections of 10 μL aliquots of these POPC vesicles. This mode of titration, i.e., lipid-into-peptide, thus does not provide the total binding enthalpy (ΔH). Since this titration experiment is unable to provide the ΔH, unlike similar titration experiments performed on other lipid membrane systems (see below for details), it was not possible for us obtain the binding isotherm from this single titration experiment.

We made an attempt to determine the ΔH by titration of the peptide solution into different POPC concentrations at very high lipid/peptide mole ratios (~50 000 to ~15 000), as employed by others (*12*, *14*). Figure 2 shows titration experiments where 10 μL aliquots of 100 μM GS14*d*K4 were injected into the reaction cell containing of 10 mM POPC (curve A) and 33.4 mM POPC (curve B). In both cases, however, the heats of the consecutive injections and the average heats of reaction were virtually identical and ΔH determined as 8.45 ± 0.05 kcal/mol. The calculations based on the measured ΔH values and the various binding models (eqs 1 and 2, see below for details) give conflicting and inconclusive results. For instance, in the case in which the peptide was titrated into 10 mM POPC, the fraction of bound peptide is found to be 63% (eq 1) and 68% (eq 2), respectively, while in the case in which peptide was titrated into 33.4 mM POPC, the fraction of bound peptide is found to be 85% (eq 1) and 88% (eq 2), respectively. It appears

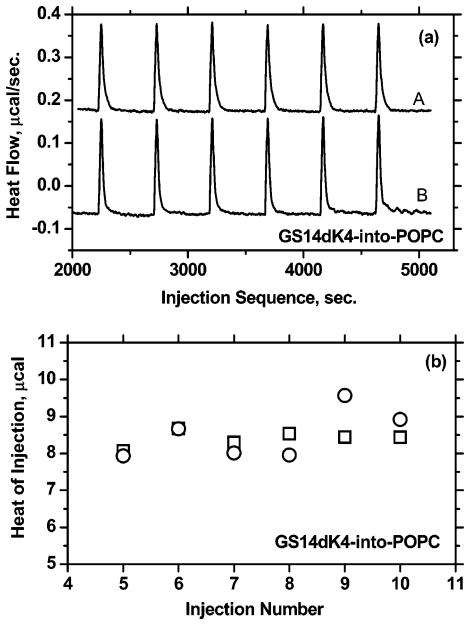

FIGURE 2: (a) ITC experimental data at 25 °C. Curve A: 10 μL aliquots of 100 μM GS14dK4 injected into the reaction cell containing 1.4448 mL of 10 mM POPC LUVs. Curve B: 10 μL aliquots of 100 μM GS14dK4 injected into the reaction cell containing 1.4448 mL of 33.4 mM POPC LUVs. (b) The heats of injection obtained by integration of the heat flow peaks as a function of injection number. Each injection produces approximately the same heat of reaction. Keys: (□) corresponds to curve A; (○) corresponds to curve B.

that in these peptide-into-lipid titrations where the lipid/peptide mole ratios are very high compared to the lipid-into-peptide titrations, binding is presumably governed by a different mechanism. Therefore, in the case of POPC lipid membranes only, we are unable to accurately obtain the binding isotherm and the ΔH value, but can only conclude that the binding of GS14*d*K4 to POPC LUVs is weak.

Binding of GS14dK4 to Charged POPG and POPS Vesicles. Figure 3a shows a titration experiment in which POPG LUVs are injected into an ITC cell containing GS14*d*K4. As evident from the titration profile, the endothermic heat flow decreases with the increase of the number of injections and the free peptide concentration in the vessel decreases simultaneously. The endothermic binding reaction essentially ceases after nine injections ($i = 9$), when all of the peptide molecules present in the reaction vessel were bound to the lipid vesicles, and the further addition of LUVs causes no further heat flow. Comparison of the individual heat release of the first injection (+43 μcal) to the cumulative heat release (+316 μcal) suggests that approximately one-eighth of the total amount of the antimicrobial peptide in the reaction cell is bound in a singe injection of the negatively charged POPG lipid vesicles. Thus, the binding appears to be very strong, which clearly demonstrates the role of the electrostatic attraction involved in the binding of the positively charged GS14*d*K4 to the oppositely charged (anionic) POPG lipid membrane. Note that GS14*d*K4 has four lysine residues and therefore has four positive charges, which in turn influences its interactions with charged lipid membranes.

Since the lipid-into-peptide titration leads to a complete binding of all peptide contained in the reaction vessel, both the total binding enthalpy (ΔH = 8.7 kcal/mol) and the

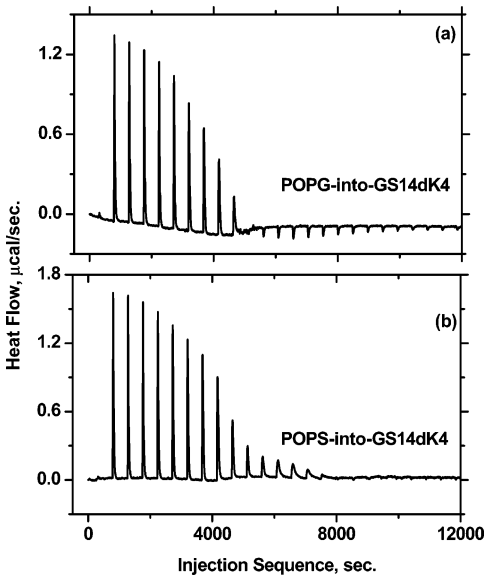

FIGURE 3: ITC experimental data at 25 °C. (a) 5 μL aliquots of 4.75 mM POPG LUVs injected into a 1.4448 mL reaction vessel containing 25 μM GS14*d*K4. The endothermic binding reaction essentially ceased after nine injections ($i = 9$) and all of the peptide molecules present in the reaction vessel appear to be bound to the lipid vesicles. (b) 5 μL aliquots of 4.0 mM POPS LUVs injected into a 1.4448 mL reaction vessel containing 25 μM GS14*d*K4. In this case, all of the peptide molecules present in the reaction vessel appear to be bound to the lipid vesicles in 14 consecutive injections.

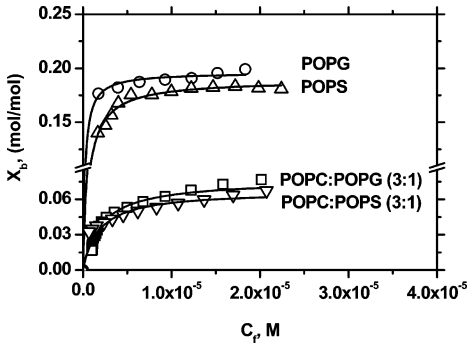

FIGURE 4: The binding isotherms of GS14*d*K4 to various single component LUVs derived from the ITC measurements at 25 °C. The degree of binding (X_b^i) is plotted as a function of free peptide concentration (c_f^i). Each data point represents an individual titration step. The solid lines represent theoretical fits according to the one-site binding model (eq 2). The dissociation constants (K_d), obtained from the theoretical fit, are summarized in Table 2. Keys: (○) POPG; (△) POPS.; (□) POPC:POPG (3:1); (▽) POPC:POPS (3:1).

binding isotherm can be obtained from the single titration experiments. The two important parameters which constitute the binding isotherm, namely, the degree of binding, X_b^i, i.e., the fraction of bound peptide per mole of total lipid, and the corresponding free peptide concentration, c_f^i, determined from the titration experiments, are shown in Figure 4. The data points represent individual titration steps. The anionic POPG lipid membrane, unlike the zwitterionic POPC membrane, is characterized by a negative surface potential. The negative surface potential drives the oppositely charged peptide to the membrane surface and facilitates the binding. With increasing amounts of bound peptide, the membrane surface potential, and therefore the electrostatic attraction, decreases. In the initial tages of binding, i.e., at higher c_f^i,

Table 2: Thermodynamic Parameters for the Binding of GS14*d*K4 to Various LUVs

systems	ΔH kcal/mol	K_c^i [a] $[M]^{-1}$	B_{max} mol/mol	K_d [M]	ΔG kcal/mol	$T\Delta S$ kcal/mol	ΔS cal/mol/K
POPG	+8.7	1.0×10^5 (at 1.7 μM)[b] 9.6×10^3 (at 21.5 μM)	0.20	2.2×10^{-7}	−11.5	+20.2	+67.8
POPS	+13.1	1.5×10^5 (0.9 μM) 8.1×10^3 (19.8 μM)	0.19	6.2×10^{-7}	−10.9	+24.0	+80.5
POPC/POPG (3:1)	+6.3	5.3×10^4 (0.6 μM) 4.0×10^3 (20.0 μM)	0.09	3.1×10^{-6}	−9.9	+16.2	+54.2
POPC/POPS (3:1)	+6.8	4.9×10^4 (0.7 μM) 3.3×10^3 (20.7 μM)	0.07	1.7×10^{-6}	−10.3	+17.1	+57.3
POPG/cholesterol (6:4)	+17.8	4.6×10^4 (0.8 μM) 6.0×10^3 (17.3 μM)	0.10	1.6×10^{-6}	−10.3	+28.1	+94.3
POPS/cholesterol (6:4)	+26.5	9.8×10^3 (0.9 μM) 3.2×10^3 (20.2 μM)	0.11	3.0×10^{-5}	−8.5	+35.0	+117.6

[a] Concentration-dependent binding constant. [b] The corresponding equilibrium peptide concentration (c_f^i) is shown in brackets.

the X_b^i decreases gradually. This is followed by a sudden drop in the X_b^i, which is characterized by a downward bending of the binding isotherm at lower c_f^i.

Under these conditions, there should be an equilibrium between the peptide in the vesicle-bound state and the peptide in the aqueous solution (free peptide). The chemical potential of the free peptide, μ_s, in solution can be written as $\mu_s = \mu_s^o + RT \ln c_f^i$, where μ_s^o is the chemical potential in the standard state. Also, the chemical potential of the membrane-bound peptide, μ_m, can be written as $\mu_m = \mu_m^o + RT \ln X_b^i$. Note that the activity coefficients are neglected from these equations for the sake of simplicity. In equilibrium, the peptide has the same chemical potential in both states (free and bound), i.e., $\mu_s = \mu_m$. Therefore, X_b^i should have a functional dependence on the c_f^i, i.e., $X_b^i = f(c_f^i)$. For practical purposes, one can obtain the concentration-dependent binding constant, K_c^i, corresponding to a particular equilibrium peptide concentration (c_f^i), directly from this binding isotherm by

$$K_c^i = \frac{X_b^i}{c_f^i} \tag{1}$$

For the present system, K_c^i varies from $K_c^i = 1.0 \times 10^5$ $[M]^{-1}$ at $c_f^i = 1.7$ μM to $K_c^i = 9.6 \times 10^3$ $[M]^{-1}$at $c_f^i = 21.5$ μM.

Attempts have been made to quantify the functional dependency, $X_b^i = f(c_f^i)$, using a one-site binding model (*15*, *16*), i.e.

$$X_b^i = \frac{B_{max} c_f^i}{K_d + c_f^i} \tag{2}$$

In this one-site binding model equation, B_{max} is the maximal binding capacity (same unit as that of X_b^i, i.e., mol/mol) and K_d is the equilibrium dissociation constant (same unit as that of c_f^i, i.e., [M]). The one-site binding model accurately describes the binding curve with a K_d of 2. 2×10^{-7} [M] (solid lines in Figure 4). Several other empirical models have also been used to describe the binding (or partitioning) of peptide to (or into) lipid bilayer membranes (*17*). In addition, there is an adsorption model based on Gouy−Chapman theory (developed on the assumption that X_b^i is linearly proportional to surface concentration of the peptide molecules), that has been used to describe the effects of the surface charge density of lipid membranes on peptide binding to lipid membrane surfaces (*12*). Considering the diversity of the model membrane systems studied (see below), we adopted an empirical model, i.e., the one-site binding model, which can accurately describe the binding isotherms generated in this study. The main purpose of using this empirical description is to obtain the dissociation constant (K_d) so that one can obtain all the relevant thermodynamic parameters and compare them among the various lipid membrane systems utilized in this study. Note that all of these empirical binding models use two or more adjustable parameters. Therefore, we do not consider the numerical values obtained from these fits as totally accurate and therefore over-interpretations of these numerical values are carefully avoided. Nevertheless, we may use the dissociation constant (K_d) to calculate the free energy of binding (ΔG) and other thermodynamic parameters and compare them among various lipid membrane systems.

The binding between the POPG membrane and GS14*d*K4 can thus be characterized thermodynamically by its K_d and ΔH. The corresponding free energy of binding, ΔG, can be calculated using the standard relation

$$\Delta G = -RT \ln\left(\frac{55.5}{K_d}\right) \tag{3}$$

where the factor 55.5 is the molar concentration of water in dilute solution that corrects for the cratic contribution to the free energy (*18*). The ΔG, i.e., the free energy change that accompanies the binding of the peptide to the lipid membrane, is determined as −11.5 kcal/mol. The value of ΔG provides a quantitative measurement of the strength of the binding such that the more negative the ΔG, the larger the degree of binding. Finally, from these thermodynamic parameters, the binding reaction entropy (ΔS) can be calculated using

$$\Delta S = \frac{(\Delta H - \Delta G)}{T} \tag{4}$$

The ΔS in this case is +67.8 cal/mole/K, which is positive, thus facilitating the binding of GS14*d*K4 to the anionic POPG membrane under these experimental conditions. Thus the binding of GS14*d*K4 to the POPG membrane is an entropy-driven process with a negative $T\Delta S$ of −20.2 kcal/mol at 25 °C, but counteracted by a positive ΔH of +8.7

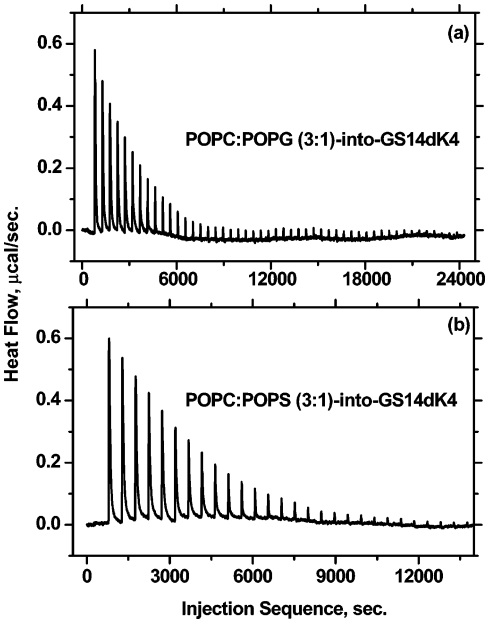

FIGURE 5: ITC experimental data at 25 °C. (a) 5 μL aliquots of 18 mM POPC/POPG (3:1) LUVs injected into a 1.4448 mL reaction vessel containing 25 μM GS14*d*K4. (b) 5 μL aliquots of 18 mM POPC/POPS (3:1) LUVs injected into a 1.4448 mL reaction vessel containing 25 μM GS14*d*K4.

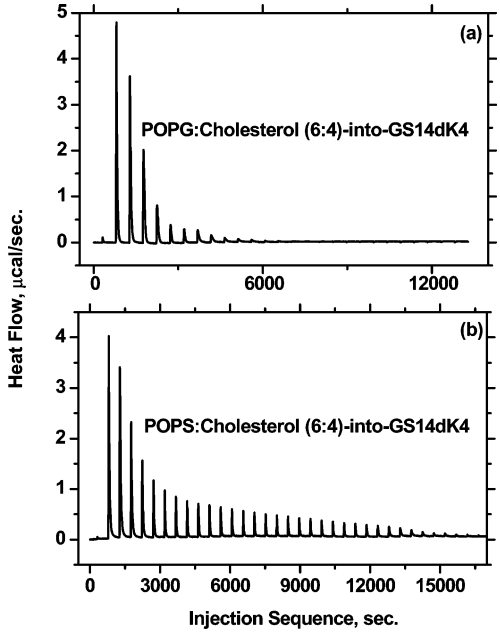

FIGURE 6: ITC experimental data at 25 °C. (a) 5 μL aliquots of 21.5 mM POPG/cholesterol (6:4) LUVs injected into a 1.4448 mL reaction vessel containing 25 μM GS14*d*K4. (b) 5 μL aliquots of 30 mM POPS/cholesterol (6:4) LUVs injected into a 1.4448 mL reaction vessel containing 25 μM, GS14*d*K4.

kcal/mol (see Table 2 for compiled thermodynamic data). The thermodynamic data are in agreement with the classical understanding of the partitioning of a nonpolar molecule from a water phase into a nonpolar phase, which is accompanied by an increase in the entropy of the system and peptide binding is thus considered to be an entropy-driven process (*19*).

Analogous to the anionic POPG lipid membrane, the anionic POPS membrane exhibits similar endothermic binding behavior to GS14*d*K4 (Figure 3b). The only notable difference is that the total endothermic binding enthalpy is found to be significantly larger than that measured for the anionic POPG system (see Table 2). However, the binding isotherm of the POPS membrane system resembles that of the POPG system (Figure 4). Moreover, the data sets corresponding to each titration step fall close to that of the POPG system. As in the case of binding of GS14*d*K4 to POPG membranes, here again the role of electrostatics is evident from the binding isotherm, and the binding process can be considered to be entropically driven but opposed by enthalpy (see Table 2). Thus, the binding process, in this case as well, follows the classical form of partitioning in the measured range of peptide concentrations.

Binding of GS14dK4 to POPC/POPG (3:1) and POPC/POPS (3:1) Mixtures. Figure 5 shows titration experiments where POPC/POPG (3:1) or POPC/POPG (3:1) LUVs were injected into an ITC cell containing GS14*d*K4 solution. The degree of binding of the positively charged GS14*d*K4 decreases significantly when three-fourth of the anionic POPG or POPS is replaced with the zwitterionic POPC (see Figure 4). The reduced degree of binding in the presence of the POPC can again be attributed to the reduced electrostatic interactions between the peptide and phospholipid bilayers. The binding isotherms of the POPC/POPG (3:1) and POPC/POPS (3:1) mixtures exhibit a close resemblance to that of the anionic lipid membranes POPG and POPS.

Binding of GS14dK4 to Lipid/Cholesterol (6:4) Mixtures. The influence of cholesterol on the binding of GS14*d*K4 to model membranes was also evaluated using ITC. The titration of 10 μL aliquots of 43 mM POPC/cholesterol (6:4) into reaction vessel containing 50 μM GS14*d*K4 shows little or no sign of peptide binding. Note that the similar titration procedure, in terms of concentrations and volumes, was used as with pure POPC membranes and that some weak binding of the peptide to POPC membrane occurs in that system (Figure 1). This finding is compatible with the role of cholesterol in reducing the lytic activity of the peptide on uncharged POPC membranes reported previously (*10*). Peptide binding, however, appears to occur to some extent in the case of anionic POPG membranes with 40 mol % cholesterol (Figure 6a). The titration data were analyzed as above and the experimentally determined binding isotherm of POPG/cholesterol (6:4) compared with that of pure POPG membrane in Figure 7. Evidently, the degree of binding of GS14*d*K4 is reduced dramatically when 40 mol % of the POPG is replaced with cholesterol. The binding isotherm as such exhibits a close resemblance to that of pure POPG LUVs. It should be emphasized that the total endothermic binding enthalpy of the peptide to the POPG/cholesterol (6:4) membrane surface is almost twice as that of the pure POPG membrane (see Table 2). This is subsequently reflected as a much larger positive entropy in the case of the POPG/cholesterol (6:4) membrane system. The titration experiments were also performed on POPS membranes containing with 40 mol % cholesterol (Figure 6b). The X_b^1 is found to be much lower than that of the POPS membrane system (Figure 7). The reduction in the degree of binding due to cholesterol is far greater than that observed for the similar POPG/cholesterol composition. Here again, the total binding enthalpy measured in POPS/cholesterol (6:4) LUVs is found to be almost twice as that of the POPS system (see Table 2).

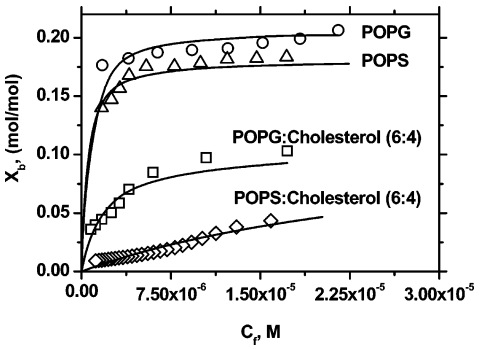

FIGURE 7: The binding isotherms of GS14*d*K4 to cholesterol containing LUVs, POPG/cholesterol (6:4) and POPS/cholesterol (6:4), derived from the ITC measurements at 25 °C. The binding isotherms of the single component LUVs, POPG and POPS, are also shown for comparison. The degree of binding (X_b^i) is plotted as a function of free peptide concentration (c_f^i). Each data point represents an individual titration step. The solid lines represent theoretical fits according to the one-site binding model (eq 2). The dissociation constants (K_d), obtained from the theoretical fit, are summarized in Table 2. Keys: (□) POPG/cholesterol (6:4); (◇) POPS/cholesterol (6:4); (○) POPG; (△) POPS.

DISCUSSION

The results presented here show that the binding of GS14*d*K4 to phospholipid bilayers is significantly influenced by the composition and specific properties of these model membranes, such as by the surface charge density and the presence or absence of cholesterol. Although some weak binding of the positively charged GS14*d*K4 occurs to the zwitterionic POPC model membranes, the degree of binding of GS14*d*K4 to the negatively charged membranes (POPG or POPS) is found to be substantially larger. Consistent with other relevant studies (*12*), a significant reduction in the degree of binding is also observed when three-fourths of the negatively charged POPG or POPS molecules are replaced with zwitterionic POPC molecules. It is interesting to note that the effects of cholesterol on the degree of binding to the charged and zwitterionic model membranes. While no measurable binding occurs in zwitterionic POPC:cholesterol LUVs, a dramatic drop in the degree of binding is observed in the charged POPG/cholesterol and POPS/cholesterol model membranes. Among these two systems, the presence of cholesterol has a much more marked influence in the POPS/cholesterol LUVs. Thus, cholesterol generally reduces the membrane affinity of the peptide, in agreement with other relevant studies (*20*−*22*). Reduced binding occurs in the presence of the cholesterol because the cholesterol molecules modify the structural properties of the bilayer as well as reducing the surface charge densities of the lipid membranes. In particular, cholesterol tightens the packing of the acyl hydrocarbon chains in the bilayer and reduces the area per lipid hydrocarbon chain (*23*).

The contribution of electrostatic attractions to the entire binding process is evident from these binding isotherms. The degree of binding increases with the increasing surface charge density of the lipid membrane, including the cholesterol-containing model membrane systems. The surface charge density determines the magnitude of electrostatic (Coulombic) attraction and the long-range electrostatic attraction drives the positively charged peptide molecules toward the negatively charged lipid membranes. The magnitude of this Coulombic attraction increases with the increasing surface charge densities of both the peptide and the lipid membrane. The Coulombic attraction also increases as the peptide approaches the membrane. In the vicinity of the membrane surface, the charged and polar groups on both the membrane and the peptide may be partially desolvated or stripped of associated water molecules, which results in the transfer of charged and polar groups of the peptide molecule from a region of high dielectric constant (aqueous solution) to a region of low dielectric constant (membrane environment). The desolvation is energetically unfavorable and may result in a repulsive interaction as the peptide comes very close to the membrane surface. The favorable hydrophobic interactions, however, mediated by hydrophobic groups of the peptide molecules, may shift the energy balance toward the penetration of the peptide molecule into polar/apolar interfacial region of the lipid membrane.

From the thermodynamic point of view, it is instructive to consider first the molecular sources of the measured overall enthalpy (ΔH). Irrespective of the model membrane system utilized, the binding reaction is found to be an endothermic process. This means that the lipid−peptide complex has a higher internal energy (E) than the individual lipid and peptide starting materials in all cases. In fact, ITC measures the overall enthalpy (heat changes) which can include (1) heat changes accompanying conformational changes in the peptide molecules; (2) heat changes associated with formation of new noncovalent bonding such as electrostatic, van der Waals and the hydrogen bonding; (3) heat changes associated with desolvation energies such as the displacement or the release of the ordered water molecules from both peptide and membrane surfaces; and (4) heat changes associated with the perturbations of the lipid membrane structure as a result of the binding. The overall enthalpy can thus be conveniently written as

$$\Delta H = (-)\Delta H_{\text{Conformation}} + (-)\Delta H_{\text{Interactions}} + (+)\Delta H_{\text{Solvation}} + (+)\Delta H_{\text{Bilayer}} \quad (5)$$

The probable contribution of changes in the conformation of GS14*d*K4 upon transfer from aqueous to membrane environment to the overall enthalpy change is difficult to estimate. Although CD, FTIR, and ^{1}H NMR spectroscopic studies have all shown that the transfer of GS14*d*K4 from aqueous to membrane or membrane mimetic environments is accompanied by an increase in β-sheet content (*9*, *11*, *24*), such studies have also shown that the conformational changes that accompany that process are relatively small. Given these observations and the fact that the formation of internal hydrogen bonds (the process driving the formation of peptide secondary structure) is generally exothermic, changes in GS14*d*K4 conformation will probably make relatively small exothermic contributions to the overall enthalpy change observed and clearly is not a major factor in the net endothermic heat changes (ΔH) measured.

The heat changes associated the formation of new noncovalent bonding such as electrostatic (Coulombic) attraction, van der Waals, and the hydrogen bonding between the peptide and membrane surfaces are exothermic in nature. However, this could be in part counteracted by the endothermic heat changes associated with the release of ordered water molecules from both the peptide and membrane

surfaces accompanying the penetration of the peptide into the lipid bilayer. The displacement of ordered water molecules is enthalpically unfavorable as it involves the breakage of hydrogen and ionic bonds.

A related plausible source of the positive enthalpy, which could in part offset the exothermic heat changes resulting from the noncovalent interactions, could originate from the consideration of the double layer theory. Note that the surfaces of both the membrane and the peptide are associated with the counterion layers which reside in the vicinity of these surfaces. The physical quantity that measures the thickness of the counterion layer is the Debye length (k^{-1}), which is inversely related to the bulk salt concentration (C_s) by $k^{-1} \propto 1/\sqrt{C_s}$. As the salt concentration increases, the electrolytes compress the thickness of this ionic layer, which results in the reduction of the Debye length (k^{-1}). According to the double layer theory, when two double layers of opposite sign overlap, the charges must neutralize each other (which must be accomplished by leaving them in pairs between the surfaces). If the charges are opposite in sign and the surface charge densities (coulomb/area) are equal in magnitude, there must be complete charge neutralization and no ion can be left unpaired in the overlapping double layers. Therefore, there must be no excess osmotic pressure at small distance of surface separation. However, if the surface charge densities on the two surfaces (and hence in the two double layers) are unequal, which very well may be the case here, there must always be an excess of charge in the overlapping double layers that cannot compensate each other exactly. Note that, for instance, on the POPG bilayer, there is an electronic charge/$\sim$68 Å^2, whereas on the surface of GS14*d*K4, there is an electronic charge/$\sim$37 Å^2. Therefore, when the surfaces come close together, there must be excess osmotic pressure due to the concentration of excess ions. This osmotic interaction is energetically unfavorable to the overall binding process and could in part offset the exothermic heat changes resulting from the noncovalent interactions between the peptide and the membrane surfaces.

An important surface phenomenon that would amount to a positive component of the enthalpy may originate from the perturbations of the lipid membrane structure or from the peptide-induced increase of the bilayer area as the peptide inserted into it (*25*−*27*). Using standard thermodynamic relations, the variations of the internal energy (E) with surface area (A) can be shown as

$$\left(\frac{\partial E}{\partial A}\right)_T = T\left(\frac{\partial S}{\partial A}\right)_T - \pi = T\left(\frac{\partial \pi}{\partial T}\right)_A - \pi \qquad (6)$$

$$\left(\frac{\partial E}{\partial A}\right)_T = T\frac{\alpha}{\chi} - \pi \qquad (7)$$

where S is the entropy, π is the surface pressure, $(\partial E/\partial A)_T$ is the internal tension, α is defined as the area expansivity at constant membrane tension, π, and χ is defined as the isothermal area compressibility or lateral compressibility. Note that the entropy term in eq 6 is replaced with a partial differential in surface pressure which follows from a two-dimensional analogue of one of Maxwell relationships. The equation becomes

$$\Delta H = \left(T\frac{\alpha}{\chi} - \pi\right)\Delta A \qquad (8)$$

Note that the volume change in the condensed phase is negligible, i.e., $\Delta H = \Delta E + \Delta(PV) \approx \Delta E$. This relation implies that the increase in surface area (ΔA) upon binding of the peptide to the bilayer surface amounts to an increase in ΔH. In addition, for relatively larger vesicles such as the ones used in this study, the isothermal area compressibility is smaller and consequently the internal tension is larger because of the relatively strong cohesive forces. Accordingly, more energy is required (or more work has to be done) to increase the surface area (or to separate the acyl chains) in the bilayer to allow for peptide penetration and binding. An interpretation can also be sought in terms lipid packing from the above eq 7. The internal tension, i.e., $(\partial E/\partial A)_T$, is larger for well-packed membranes because of the relatively strong cohesive forces that exist in such membranes. Therefore, relatively more energy is required or more work has to be done for peptide binding in the more well ordered lipid membranes. The irregular contour of GS14*d*K4 may not pack as well with the surrounding lipid molecules and therefore the replacement of lipid−lipid molecular interactions with lipid−protein interactions, especially in more well ordered membrane systems, may lead to relatively higher endothermic enthalpies (ΔH).

Having considered the possible molecular sources of the positive enthalpy, let us turn our attention to the overall binding enthalpy measured for different lipid membrane systems. We find that the measured overall binding enthalpy varies markedly with variations in lipid membrane compositions. Specifically, the overall enthalpy decreases in the following order (Table 2): POPS/cholesterol (6:4) $\gg$ POPG/cholesterol (6:4) $\gg$ POPS $\gg$ POPG > POPC/POPS (3:1) $\geq$ POPC/POPG (3:1). A pronounced positive binding enthalpy is noticeable, especially in POPS- and cholesterol-containing lipid membranes. This dramatic variation among various model membranes may be explained solely from the point of view of the packing and the order of these membrane systems. Among the single-component membrane systems, considering the gel−liquid crystalline transition temperatures, the POPS membrane is more ordered than the POPG membrane at 25 °C (experimental temperature). This is reflected as the relatively higher endothermic enthalpy of peptide binding in the case of POPS membranes. The binary lipid mixtures, POPC/POPG (3:1) and POPC/POPS (3:1), are likely to be more disordered than their counterparts and therefore less energy is required for the peptide binding. The presence of cholesterol also has a significant effect on the enthalpy of binding. The binding enthalpies of POPG/cholesterol (6:4) and POPS/cholesterol (6:4) systems are as much as twice those measured for their respective pure lipid systems. It is well accepted that the incorporation of cholesterol in lipid membranes results in increased membrane cohesion and more highly ordered hydrocarbon chains because cholesterol tightens the packing of hydrocarbon chains in the bilayer or decreases the area per lipid hydrocarbon chain (*28*). The cohesion between lipid molecules, which is experimentally measured as the bilayer area compressibility modulus from stress−strain plots, is found to increase with increasing cholesterol content (*28*). Because of the tight packing and the increased membrane cohesion in the presence of the cholesterol, more work or more energy is required to separate the acyl hydrocarbon chains in the bilayer to allow for the peptide penetration and binding. This

is eventually reflected as a much larger positive contribution to the overall endothermic enthalpy in the cholesterol-containing lipid membrane systems.

As detailed above, GS14*d*K4 binds to all the lipid membranes studied with endothermic reaction enthalpies. Therefore, the negative free energy ($\Delta G = -RT \ln [55.5/K_d]$), which is calculated from one-site binding model, must originate from sufficiently large positive entropy changes such that $T\Delta S$ more than compensates the positive binding enthalpy (ΔH). Thus, the binding of GS14*d*K4 to lipid membranes follows the classical hydrophobic effect, which is an entropically driven process. The negative free energy, which is determined from the binding constant, remains nearly the same (i.e., $\Delta G = -9.9$ to -11.5 kcal/mol) for all anionic and anionic-zwitterionic lipid membrane systems, including the cholesterol constituted membranes, with the exception of POPS/cholesterol (6:4) system ($\Delta G = -8.4$ kcal/mol). A relatively small variation of negative free energy (from -8.4 to -11.4 kcal/mol), together with a pronounced variation of positive enthalpy (from $+6.3$ to $+26.5$ kcal/mol), leads to an equally strong variation of $T\Delta S$ (from $+16.2$ to $+34.8$ kcal/mol). The entropy change ($T\Delta S$) accompanying peptide binding thus decreases in the same order as of the binding enthalpy (Table 2): POPS/cholesterol (6:4) $\gg$ POPG/cholesterol (6:4) $\gg$ POPS $\gg$ POPG $>$ POPC/POPS (3:1) $\geq$ POPC/POPG (3:1). Therefore, the formation of the lipid−protein complex, which is enthalpically unfavorable, proceeds in the forward direction due to the favorable entropy change caused by the disordering of the lipid membrane systems.

One may also explain the entropy increase accompanied by the peptide binding from the above thermodynamic relations

$$T\left(\frac{\partial S}{\partial A}\right)_T = T\left(\frac{\partial \pi}{\partial T}\right)_A = T\frac{\alpha}{\chi} \quad (9)$$

$$T\Delta S = T\left(\frac{\alpha}{\chi}\right)\Delta A \quad (10)$$

These thermodynamic relations imply that the increase in surface area (ΔA) of the bilayer upon binding of the peptide to the bilayer surface, which is accompanied by adsorption of heat ($+\Delta H$), also leads to an proportionally large entropy increase ($T\Delta S$) due to the disordering of the acyl hydrocarbon chains. Thus, the peptide-induced area increase of the bilayer structure, which subsequently causes the increase in the disorder of the bilayer phase, is a primary driving force for the peptide binding to these relatively planar membrane systems.

REFERENCES

1. Prenner, E. J., Lewis, R. N. A. H., and McElhaney, R. N. (1999) The interaction of the antimicrobial peptide gramicidin S with lipid bilayer and biological membranes. *Biochim. Biophys. Acta 1462*, 201−221.
2. Hancock, R. E., and Chapple, D. S. (1999) Peptide antibiotics, *Antimicrob. Agents Chemother. 43*, 1317−1323.
3. Waki, M., and Izumiya, N. (1990) Chemical synthesis and bioactivity of gramicidin S and related peptides, in *Biochemistry of Peptide Antibiotics: Recent Advances in the Biotechnology of β-Lactams and Bioactive Peptides* (Kleinkauff, H., and van Dohren, H., Eds.) pp 205−240, Walter de Gruyter and Company, Berlin.
4. Kondejewski, L. H., Farmer, S. W., Wishart, D. S., Hancock, R. E. W., and Hodges, R. H. (1996) Gramicidin S is active against both Gram-positive and Gram-negative bacteria, *Int. J. Peptide Protein Res. 47*, 460−466.
5. Kondejewski, L. H., Farmer, S. W., Wishart, D. S., Kay, C. M., Hancock, R. E. W., and Hodges, R. H. (1996) Modulation of structure and antibacterial and hemolytic activity by ring size in cyclic gramicidin S analogs, *J. Biol. Chem. 271*, 25261−25268.
6. Kondejewski, L. H., Jelokhani-Niaraki, M., Farmer, S. W., Lix, B., Kay, C. M., Sykes, B. D., Hancock, R. E. W., and Hodges, R. S. (1999) Dissociation of antimicrobial and hemolytic activities in cyclic peptide diastereomers by systematic alterations in amphipathicity, *J. Biol. Chem. 274*, 13181−13192.
7. Jelokhani-Niaraki, M., Kondejewski, L. H., Farmer, S. W., Hancock, R. E. W., Kay, C. M., and Hodges, R. S. (2000) Diastereoisomeric analogues of gramicidin S: Structure, biological activity and interaction with lipid bilayers, *Biochem. J. 349*, 747−755.
8. Lee, D. L., Mant C. T., and Hodges R. S. (2003). A novel method to measure self-association of small amphipathic molecules: Temperature profiling in reversed-phase chromatography. *J. Biol. Chem. 278*, 22918−22927.
9. Lewis, R. N. A. H., Kiricsi, M., Prenner, J., Hodges, R. S., and McElhaney R. N. (2003) Fourier transform infrared spectroscopic study of the interactions of a strongly antimicrobial but weakly hemolytic analogue of gramicidin S with lipid micelles and lipid bilayer membranes, *Biochemistry 42*, 440−449.
10. Prenner, E. J., Lewis, R. N. A. H., Jelokhani-Niaraki, M., Hodges R. S., and McElhaney, R. N. (2001) Cholesterol attenuates the interaction of the antimicrobial peptide gramicidin S with phospholipid bilayer membranes, *Biochim. Biophys. Acta 1510*, 83−92.
11. Jelokhani-Niaraki, M., Prenner, E. J., Kondejewski, L. H., Kay, C. M., McElhaney, R. N., and Hodges, R. S. (2001) Conformations and interactions of cyclic cationic antimicrobial peptides in lipid bilayers, *J. Peptide Res. 60*, 23−36.
12. Wieprecht, T., and Seelig, J. (2002) Isothermal titration calorimetry for studying interactions between peptides and lipid membranes, *Curr. Top. Membr. 52*, 31−56.
13. Wiseman, T., Williston, S., Brandts, J. F., and Lin, L. N. (1989) Rapid measurement of binding constants and heats of binding using a new titration calorimeter, *Anal. Biochem. 17*, 131−137.
14. Saito, H., Dhanasekaran, P., Baldwin, F., and Weisgraber, K. H. (2001) Lipid binding-induced conformational change in human apolipoprotein E, *J. Biol. Chem. 276*, 40949−54.
15. van Holde, K. E. (1971) *Physical Biochemistry*, Chapter 3, Prentice Hall, Inc., Eaglewood Cliffs, New Jersey.
16. Bowden, A. C. (1976) *Principles of Enzyme Kinetics*, Butterworths, London.
17. White, S. H., Wimley, W. C., Ladokhin, A. S., Hristova, K. (1998) Protein folding in membranes: Determining energetcis of peptide-bilayer interactions, *Methods Enzymol. 295*, 62−87.
18. Cantor C. R., and Schimmel, P. R. (1980) *Biophysical Chemistry Part I: The Conformation of Biological Macromolecules*, Chapter 5, W. H. Freeman and Company, San Francisco.
19. Tanford C. (1980) *The Hydrophobic Effects*, John Wiley & Sons, Inc., New York.
20. Allende, D., Vidal, A., and McIntosh T. J. (2002) Jumping to rafts: Gatekeeper role of bilayer elasticity, *Trends Biochem. Sci. 29*, 325−330.
21. Wieprecht T., Beyermann, M., and Seelig J. (1999) Binding of antibacterial magainin peptides to electrically neutral membranes: Thermodynamics and structure, *Biochemistry 38*, 10377−10387.
22. McIntosh T. J., Vidal, A., and Simon, S. A. (2002) The energetics of peptide-lipid interactions: Modulation by interfacial dipoles and cholesterol, *Curr. Top. Membr. 52*, 309−338.
23. Lecuyer, H., and Dervichian, D. G. (1969) Structure of aqueous mixtures of lecithin and cholesterol, *J. Mol. Biol. 45*, 39−57.
24. McInnes, C., Kondejewski, L. H., Hodges, R. S., and Sykes, B. D. (2000) Development of the structural basis for antimicrobial and hemolytic activities of peptides based on gramicidin S and design of novel analogs using NMR spectroscopy, *J. Biol. Chem. 275*, 14287−14297.

25. Beschiaschvili, G., and Seelig, J. (1992) Peptide binding to lipid bilayers: Nonclassical hydrophobic effect and membrane-induced p*K* shifts, *Biochemistry 31*, 10044−10053.
26. Bloom, M., Evans, E., and Mouritsen, O. G. (1991) Physical properties of the fluid lipid-bilayer component of cell membranes: a perspective, *Q. Rev. Biophys. 24*, 293−397.
27. Davies, R. J., and Jones, M. N. (1992) The thermal behaviour of phosphatidylcholine-glycophorin monolayers in relation to monolayer and bilayer internal pressure, *Biochim. Biophys. Acta 1103*, 8−12.
28. Needham, D., and Nunn, R. S. (1990) Elastic deformation and failure of lipid bilayer membranes containing cholesterol. *Biophys. J. 58*, 997−1009.

BI048077D